AMERICAN SOCIETY FOR MICROBIOLOGY | mBio®

RESEARCH ARTICLE
Clinical Science and Epidemiology

Population Structure, Molecular Epidemiology, and β-Lactamase Diversity among *Stenotrophomonas maltophilia* Isolates in the United States

Maria F. Mojica,[a,b]* Joseph D. Rutter,[b] Magdalena Taracila,[b,c] Luciano A. Abriata,[d,e] Derrick E. Fouts,[f] Krisztina M. Papp-Wallace,[a,b,c] Thomas J. Walsh,[g] John J. LiPuma,[h] Alejandro J. Vila,[i] Robert A. Bonomo[j,k,l,m,n,o,p,q]

[a]Department of Biochemistry, Case Western Reserve University School of Medicine, Cleveland, Ohio, USA
[b]Research Service, Louis Stokes Veterans Affairs Medical Center, Cleveland, Ohio, USA
[c]Department of Medicine, Case Western Reserve University School of Medicine, Cleveland, Ohio, USA
[d]Laboratory for Biomolecular Modeling, Institute of Bioengineering, School of Life Sciences, École Polytechnique Fédérale de Lausanne, Lausanne, Switzerland
[e]Swiss Institute of Bioinformatics, Lausanne, Switzerland
[f]J Craig Venter Institute, Rockville, Maryland, USA
[g]Transplantation Oncology Infectious Diseases Program, Weill Cornell Medical Center, New York, New York, USA
[h]Department of Pediatrics, University of Michigan Medical School, Ann Arbor, Michigan, USA
[i]Instituto de Biología Molecular y Celular de Rosario (IBR, CONICET-UNR), Rosario, Argentina
[j]Department of Medicine, Case Western Reserve University School of Medicine, Cleveland, Ohio, USA
[k]Department of Pharmacology, Case Western Reserve University School of Medicine, Cleveland, Ohio, USA
[l]Department of Molecular Biology and Microbiology, Case Western Reserve University School of Medicine, Cleveland, Ohio, USA
[m]Department of Biochemistry, Case Western Reserve University School of Medicine, Cleveland, Ohio, USA
[n]Center for Proteomics and Bioinformatics, Case Western Reserve University School of Medicine, Cleveland, Ohio, USA
[o]Medical Service, Louis Stokes Cleveland Veterans Affairs Medical Center, Cleveland, Ohio, USA
[p]GRECC, Louis Stokes Cleveland Veterans Affairs Medical Center, Cleveland, Ohio, USA
[q]CWRU-Cleveland VAMC Center for Antimicrobial Resistance and Epidemiology (Case VA CARES), Cleveland, Ohio, USA

ABSTRACT *Stenotrophomonas maltophilia* is a Gram-negative, nonfermenting, environmental bacillus that is an important cause of nosocomial infections, primarily associated with the respiratory tract in the immunocompromised population. Aiming to understand the population structure, microbiological characteristics and impact of allelic variation on β-lactamase structure and function, we collected 130 clinical isolates from across the United States. Identification of 90 different sequence types (STs), of which 63 are new allelic combinations, demonstrates the high diversity of this species. The majority of the isolates (45%) belong to genomic group 6. We also report excellent activity of the ceftazidime-avibactam and aztreonam combination, especially against strains recovered from blood and respiratory infections for which the susceptibility is higher than the susceptibility to trimethoprim-sulfamethoxazole, considered the "first-line" antibiotic to treat *S. maltophilia*. Analysis of 73 bla_{L1} and 116 bla_{L2} genes identified 35 and 43 novel variants of L1 and L2 β-lactamases, respectively. Investigation of the derived amino acid sequences showed that substitutions are mostly conservative and scattered throughout the protein, preferentially affecting positions that do not compromise enzyme function but that may have an impact on substrate and inhibitor binding. Interestingly, we detected a probable association between a specific type of L1 and L2 and genomic group 6. Taken together, our results provide an overview of the molecular epidemiology of *S. maltophilia* clinical strains from the United States. In particular, the discovery of new L1 and L2 variants warrants further study to fully understand the relationship between them and the β-lactam resistance phenotype in this pathogen.

Citation Mojica MF, Rutter JD, Taracila M, Abriata LA, Fouts DE, Papp-Wallace KM, Walsh TJ, LiPuma JJ, Vila AJ, Bonomo RA. 2019. Population structure, molecular epidemiology, and β-lactamase diversity among *Stenotrophomonas maltophilia* isolates in the United States. mBio 10:e00405-19. https://doi.org/10.1128/mBio.00405-19.

Editor Steven J. Projan, MedImmune

This is a work of the U.S. Government and is not subject to copyright protection in the United States. Foreign copyrights may apply.

Address correspondence to Robert A. Bonomo, Robert.Bonomo@va.gov.

* Present address: Maria F. Mojica, Grupo de Investigación en Resistencia Antimicrobiana y Epidemiología Hospitalaria–RAEH, Universidad El Bosque, Bogotá, Colombia.

Received 13 February 2019
Accepted 3 June 2019
Published 2 July 2019

Downloaded from http://mbio.asm.org/ on April 15, 2021 by guest

IMPORTANCE Multiple antibiotic resistance mechanisms, including two β-lactamases, L1, a metallo-β-lactamase, and L2, a class A cephalosporinase, make *S. maltophilia* naturally multidrug resistant. Thus, infections caused by *S. maltophilia* pose a big therapeutic challenge. Our study aims to understand the microbiological and molecular characteristics of *S. maltophilia* isolates recovered from human sources. A highlight of the resistance profile of this collection is the excellent activity of the ceftazidime-avibactam and aztreonam combination. We hope this result prompts controlled and observational studies to add clinical data on the utility and safety of this therapy. We also identify 35 and 43 novel variants of L1 and L2, respectively, some of which harbor novel substitutions that could potentially affect substrate and/or inhibitor binding. We believe our results provide valuable knowledge to understand the epidemiology of this species and to advance mechanism-based inhibitor design to add to the limited arsenal of antibiotics active against this pathogen.

KEYWORDS *Stenotrophomonas maltophilia*, antibiotic resistance, beta-lactamases, molecular epidemiology

Stenotrophomonas maltophilia is a nonfermentative, Gram-negative, environmental bacillus that has emerged as an important cause of health care-associated infections (HCAIs), especially in debilitated and immunocompromised patients. In persons with cystic fibrosis (CF), *S. maltophilia* is known for colonizing the airways and causing chronic infections (1, 2). Although *S. maltophilia* is primarily associated with respiratory tract infections, this pathogen can cause a wide range of clinical syndromes, including bloodstream, catheter-associated, and skin and soft tissue infections (2–4). Furthermore, while *S. maltophilia* is not a highly virulent pathogen, its associated crude mortality rates range from 14% to 69% in patients with bacteremia (1, 5–8). Recognized risk factors for *S. maltophilia* infection include underlying malignancy, the presence of indwelling devices, chronic respiratory disease, prior use of antibiotics (particularly imipenem or meropenem), and long-term hospitalization or intensive care unit admission. These risk factors reflect the tendency of *S. maltophilia* to form biofilms and colonize humid surfaces and its multidrug-resistant (MDR) phenotype (2, 9).

S. maltophilia is recognized by the World Health Organization as one of the leading MDR organisms in hospital settings for which disease prevention and treatment strategies must be developed (10). In *S. maltophilia*, intrinsic antibiotic resistance is mediated by the expression of aminoglycoside-modifying enzymes, *qnrB*-like quinolone-resistant determinants, multidrug efflux pumps, and two inducible β-lactamases, L1 and L2. L1 is a class B3 metallo-β-lactamase (MBL) that hydrolyzes carbapenems and other β-lactams, with the important exception of the monobactam aztreonam (ATM), and is resistant to all clinically available β-lactamase inhibitors (1, 11, 12). L2 is a class A cephalosporinase that confers resistance to extended-spectrum cephalosporins and ATM but can be inhibited by commercially available serine-β-lactamase inhibitors such as clavulanic acid and avibactam (1, 2, 13, 14). Infections with *S. maltophilia* isolates demonstrating resistance to antibiotics with historically good susceptibility rates, such as trimethoprim-sulfamethoxazole (TMP-SMX), ticarcillin-clavulanate (TIC-CLV), and fluoroquinolones, are increasingly common (2, 5, 15, 16). Moreover, resistance can also emerge during therapy (14, 15).

The genetic background of *S. maltophilia* strains was previously explored using various molecular methods, including pulsed-field gel electrophoresis (PFGE), amplified fragment length polymorphism (AFLP), and recently by multilocus sequence typing (MLST). These methods demonstrated a high level of molecular heterogeneity, which may be related to the wide environmental distribution of this pathogen (17–20). Furthermore, allelic variation of the bla_{L1} and bla_{L2} genes has also been recognized (21). The implications of such molecular heterogeneity in β-lactamase function and the resistance phenotypes that they might confer have not been fully explored and are essential to anticipate emergence of antibiotic resistance and novel phenotypes.

Downloaded from http://mbio.asm.org/ on April 15, 2021 by guest

TABLE 1 Antimicrobial susceptibility rate of 130 clinical *S. maltophilia* isolates according to CF status and type of clinical specimen[a]

	CF isolates (n = 49)			Blood isolates (n = 28)			Isolates from other infections[b] (n = 34)			Stool isolates (n = 16)		
		MIC (mg/liter)			MIC (mg/liter)			MIC (mg/liter)			MIC (mg/liter)	
Antimicrobial	% S	MIC_{50}	MIC_{90}	% S	MIC_{50}	MIC_{90}	% S	MIC_{50}	MIC_{90}	% S	MIC_{50}	MIC_{90}
CIP[c]	29	2	>16	25	2	>16	38	2	16	43	2	8
TMP-SMX	96	1	2	79	1	4	82	1	4	100	1	1
MIN	98	≤2	≤2	100	≤2	≤2	100	≤2	≤2	100	≤2	≤2
ATM[c]	0	>256	>256	0	256	>256	0	>256	>256	0	>256	>256
CAZ	16	64	>256	43	16	256	15	128	256	19	64	128
TIC-CLV	24	64	>256	25	32	128	18	64	256	19	32	256
CZA	12	64	>256	36	16	256	18	128	256	38	64	128
CZA (4 mg/liter)-ATM (4 mg/liter)	69	0.125	>32	100	≤0.06	≤0.06	76	≤0.06	≤0.06	100	≤0.06	≤0.06
CZA (4 mg/liter)-ATM (8 mg/liter)	96	≤0.06	≤0.06	100	≤0.06	≤0.06	94	≤0.06	≤0.06	100	≤0.06	≤0.06

[a]CIP, ciprofloxacin; TMP-SMX, trimethoprim-sulfamethoxazole; MIN, minocycline; ATM, aztreonam; CAZ, ceftazidime; TIC-CLV, ticarcillin-clavulanate; CZA, ceftazidime-avibactam; CZA-ATM, ceftazidime-avibactam and aztreonam. % S, % susceptibility.
[b]Includes isolates recovered from respiratory samples (n = 24), wounds/abscesses (n = 5), urinary tract (n = 3), and eyes/contact lens (n = 2).
[c]CLSI breakpoints for *P. aeruginosa* were used.

Using clinical strains from a very diverse collection, we explored the genetic population structure, antibiotic resistance profiles, and allelic variation of the *bla* genes of clinical *S. maltophilia* strains collected across the United States. Our goal was to understand the impact of allelic variation on β-lactamase structure and function as a first step in probing the sequence, structure, functionality, and stability that give rise to a particular β-lactam-resistant phenotype in this pathogen.

RESULTS

Clinical characteristics of the isolates. The geographical distribution of the isolates included in the study is presented in Fig. S1 in the supplemental material. From the 130 strains included, 38% (49/130) originated from patients with CF. Of the 81 strains recovered from non-CF individuals, the majority were collected from blood samples (35%; 28/81), followed by respiratory samples (29%; 24/81); other sites of isolation, including eyes/contact lenses, urinary tract, and wounds/abscess, accounted for 12% (10/81) of these specimens. Nineteen percent of the strains (16/81) were collected from rectal swabs.

Antimicrobial susceptibility determinations are summarized in Table 1 according to clinical status and type of specimen. Intermediate and resistant strains were further grouped together into a nonsusceptible category. The full susceptibility profile of isolates included in this study can be found in Dataset S1 in the supplemental material.

Genotypic characterization. MLST of the 130 strains demonstrated that they belonged to 90 different sequence types (STs), of which 27 were known STs and 63 are novel STs. All new alleles were deposited on the *S. maltophilia* MLST website (https://pubmlst.org/smaltophilia/). The most common ST found was ST5 (n = 9), followed by ST77 (n = 7). Clonal analysis using eBURST v3, with a clonal group defined as isolates sharing 5 identical loci, identified 8 distinct clonal groups as follows: group 1, ST193, ST213, ST221, and ST231; group 2, ST211, ST234, and ST246; group 3, ST26, ST27, and ST162; group 4, ST224 and ST235; group 5, ST29 and ST219; group 6, ST119 and ST208; group 7, ST23 and ST233; and group 8, ST77 and ST243. Additionally, this analysis identified 71 singleton STs.

A phylogenetic tree constructed with the concatenated sequences of the seven housekeeping genes used in the MLST scheme is shown in Fig. 1. Previously assigned STs of genomic group 6, namely ST4, ST5, ST26, ST27, ST28, and ST31, clustered together with 31 newly assigned STs, representing 45.4% of all isolates. Similarly, ST29 from genomic group C, ST23 and ST24 from genomic group 1, and ST39 from genomic group 4 clustered with 10, 8, and 1 newly assigned STs, respectively. Thus, these genomic groups represent 13%, 14%, and 1.5% of the isolates. Fifty-six isolates did not

Downloaded from http://mbio.asm.org/ on April 15, 2021 by guest

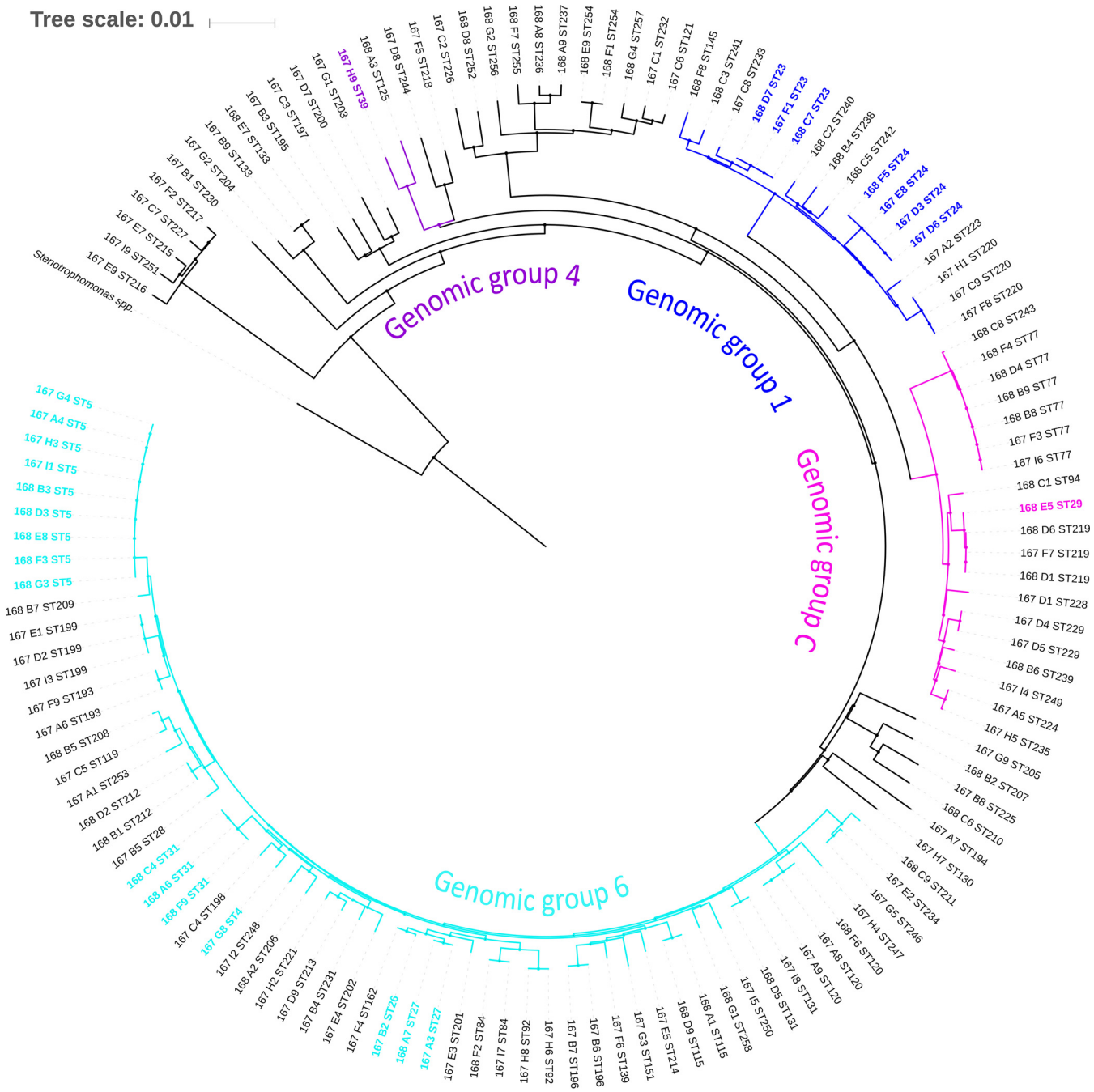

FIG 1 Phylogenetic analysis of *S. maltophilia* from concatenated sequences of the seven housekeeping gene fragments (3,591 nt). Consensus UPGMA tree shows the structure of the studied *S. maltophilia* population ($n = 130$). Branch length represents the genetic distance, with the scale bar indicating the number of mutations per nucleotide position. The tree was rooted with a sequence from *Stenotrophomonas* spp. (not *S. maltophilia*). The genomic group affiliation according to MLST in the original study by Kaiser et al. (20) is indicated by colored clades: cyan, genomic group 6; blue, genomic group 1; purple, genomic group 4; magenta, genomic group C. Known STs belonging to each genomic group are highlighted in their corresponding color.

cluster with any known ST from a previously reported genomic group, possibly indicating the emergence of new genomic groups. Interestingly, clustering of strains was not observed according to their geographical location, physiological site of isolation, or CF/clinical status (Fig. S2).

L1 and L2 β-lactamase characterization. Sequences of bla_{L1} were obtained for 73 out of 130 isolates included (56%). Using primers Smal_L1_F and Smal_L1_R, bla_{L1} was successfully detected in 27 of the remaining 56 isolates. Therefore, bla_{L1} could not be

Downloaded from http://mbio.asm.org/ on April 15, 2021 by guest

detected in 29 samples (22%), probably due to sequence variation of the target. On the other hand, bla_{L2} was successfully sequenced in 116 of the 130 clinical isolates (89%) and detected in 12 of the 14 remaining isolates. Analysis of the coding sequences showed a higher degree of variability in the third codon position than in the first and second positions, by factors of 2 to 4 (Fig. S3). Mutations at position 3 (wobble position) often do not imply a change in the encoded amino acid (and those that do result in amino acid changes tend to conserve physicochemical properties). Overall, the two data sets display relatively high amino acid conservation (compared to examples of natural [22] or lab-generated [23] variation in enzymes), with most positions accepting substitutions by at most 5 amino acid residues different from the reference sequence. Analysis of amino acid residue preferences shows that substitutions largely conserve patterns of residue volume, steric hindrance, flexibility, polarity, and side chain charge. Examples of these conservative amino acid substitutions include Ala77Ser, Val133Leu, and Lys212Arg in L1 and (Val/Leu)169Met, Thr126Ala, and Glu197Asp in L2 (Dataset S1).

Multiple sequence alignment (MSA) of the deduced amino acid sequences of the mature protein (268 amino acids, starting from the EA/T/VPLP sequence after the predicted signal peptide of L1; and 276 or 277 amino acids, starting from the VSP sequence after the predicted signal peptide of L2) and a subsequent protein sequence logo showed that substitutions are scattered throughout the protein (Fig. S4). A sequence logo was further used to identify positions in which two, three, four, or more different residues were found. Mapping of these positions onto the crystal structures of the L1 monomer (PDB ID 2AIO), L1 homotetramer (PDB ID 2QIN), and L2 (PDB ID 1N4O) is shown in Fig. 2.

A dendrogram was then built with all 73 clinical L1 sequences, the 5 reference sequences described by Avison et al. (21), and the amino acid sequence of the FEZ-1 MBL of *Legionella gormanii* as the outgroup. As shown in Fig. 3, sequences grouped into four distinct clades, identified by different colors. The majority of clinical L1 enzymes were identical, with 100% amino acid identity (34 sequences, 46.6%), or highly related, with >85% amino acid identity (2 sequences, 2.7%), to the reference L1 B (red clade). Reference L1 C clustered with seventeen clinical L1 enzymes (23.3%), of which two were identical to this reference (green clade). References L1 A and L1 D clustered together with seven clinical L1s, representing 10% of the sequences (blue clade), while reference L1 E clustered with seven clinical L1s. Finally, three L1 clinical sequences were not grouped into any clade.

On the other hand, the dendrogram built using all 116 L2 sequences obtained from the clinical isolates, the four L2 (A to D) reference sequences described by Avison et al. (21), and the amino acid sequence of *Klebsiella pneumoniae* carbapanemase KPC-2 as the outgroup clearly divided the L2 clinical sequences into two distinct clades (Fig. 4). References L2 A, L2 B, and L2 C grouped with the majority of the clinical L2s (67 sequences; 57.8%) into the brown clade. This clade branches out into two clades: the first clusters 59 identical clinical L2s (18 sequences; 15.5%) or highly related L2s (33 sequences; 28.4%) to the L2 B reference, whereas the other branch groups references L2 A and L2 C with the remaining 8 sequences. The green clade clusters 47 clinical L2s (40.5%) with reference L2 D. This clade branches out into 4 clades.

Further MSAs carried out with the sequences of each clade helped identify repeated sequences, as well as unique L1 and L2 variants. A comparison with the reference types identified unique substitutions yielding 34 new variants of the L1 MBL and 43 new variants of L2, with percent identities ranging from 78% to 99% and from 58% to 99%, respectively (Fig. S5). A list of all the substitutions found in the clinical isolates is shown in Tables S1 and S2.

Finally, BIS2Analyzer was used to analyze amino acid variation within L1 and L2 variants. This is a server-based program tailored to detect residue covariation in highly conserved alignments and thus identify protein regions that might not be essential for function but do contribute to relevant aspects of structure and function (hence they are not strictly conserved but not fully tolerant of substitutions). Among the unique-sequence L1 variants, BIS2Analyzer detected two clusters of covarying residues, which

Downloaded from http://mbio.asm.org/ on April 15, 2021 by guest

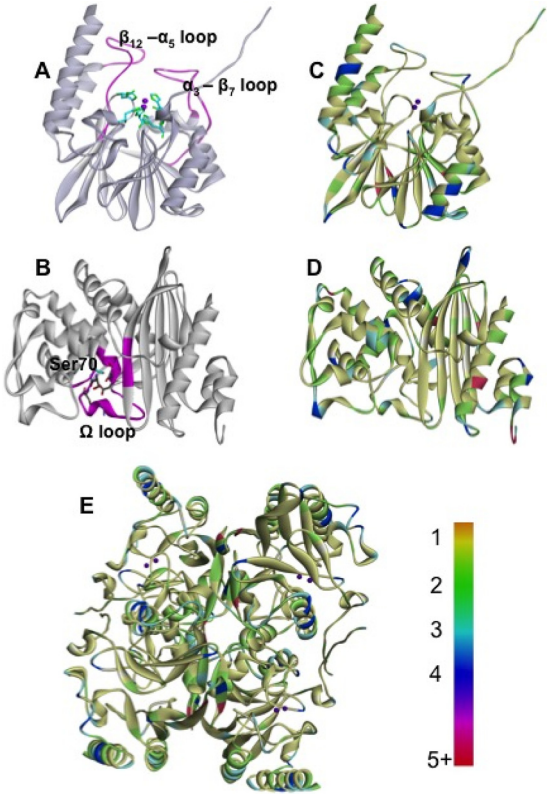

FIG 2 Protein structure and amino acid variability in the L1 and L2 β-lactamases. (A) Structure of L1 (PDB ID 2IOA) displaying the Zn-binding residues as cyan sticks, Zn ions as purple spheres, and mobile loops in magenta. (B) Structure of L2 (PDB ID 1N4O) displaying important catalytic residues in sticks with Ser70 highlighted in cyan and the Ω-loop in magenta. (C and D) Amino acid variability in the L1 (C) and L2 (D) enzymes. Sequences obtained from 130 clinical strains and their reference sequences previously described by Avison et al. (21) were aligned, and variability per residue is indicated by the color scale shown at the bottom right from a conserved position (yellow) to a position where two (green), three (cyan), four (blue), or five or more (magenta) different amino acids can be found. (E) Mapping of amino acid variability in the crystal structure of the L1 tetramer (PDB ID 2QIN).

were mapped onto the crystal structure of the monomer (PDB ID 2AIO) and tetramer (PDB ID 2QIN) in Fig. 5. The analysis revealed that strictly conserved residues involved in zinc binding and in tetramerization were surrounded by residues that tolerate substitution, but under covariation constraints. The cluster highlighted in green in Fig. 5 arises from covariation of residues surrounding zinc-binding residues and Met175, a residue key for tetramerization (24). The cluster highlighted in blue contains additional covarying residues that map to the tetramerization interfaces.

On the unique amino acid sequences of L2 variants, Bis2Analyzer identified a single cluster of residues that tolerate substitutions under covariation constraints. Figure 6 shows that residues of this network are scattered throughout most of the structure, enriched around the active site and in the Ω-loop.

DISCUSSION

In this compilation of *S. maltophilia* clinical strains, collected over a 10-year period across the United States, we found that the majority (56%) of isolates were recovered from persons with CF or from respiratory samples, 21% of the strains were recovered from blood, and minor percentages were recovered from urine (2.3%) and soft tissue infections (3%). Although the predominance of respiratory samples is consistent with other studies, the small sample size prevents us from drawing any conclusion regarding human infection preference.

Antibiotic agents with *in vitro* activity against *S. maltophilia* include TMP-SMX, fluoroquinolones, aminoglycosides, and extended-spectrum penicillins/cephalosporins

Downloaded from http://mbio.asm.org/ on April 15, 2021 by guest

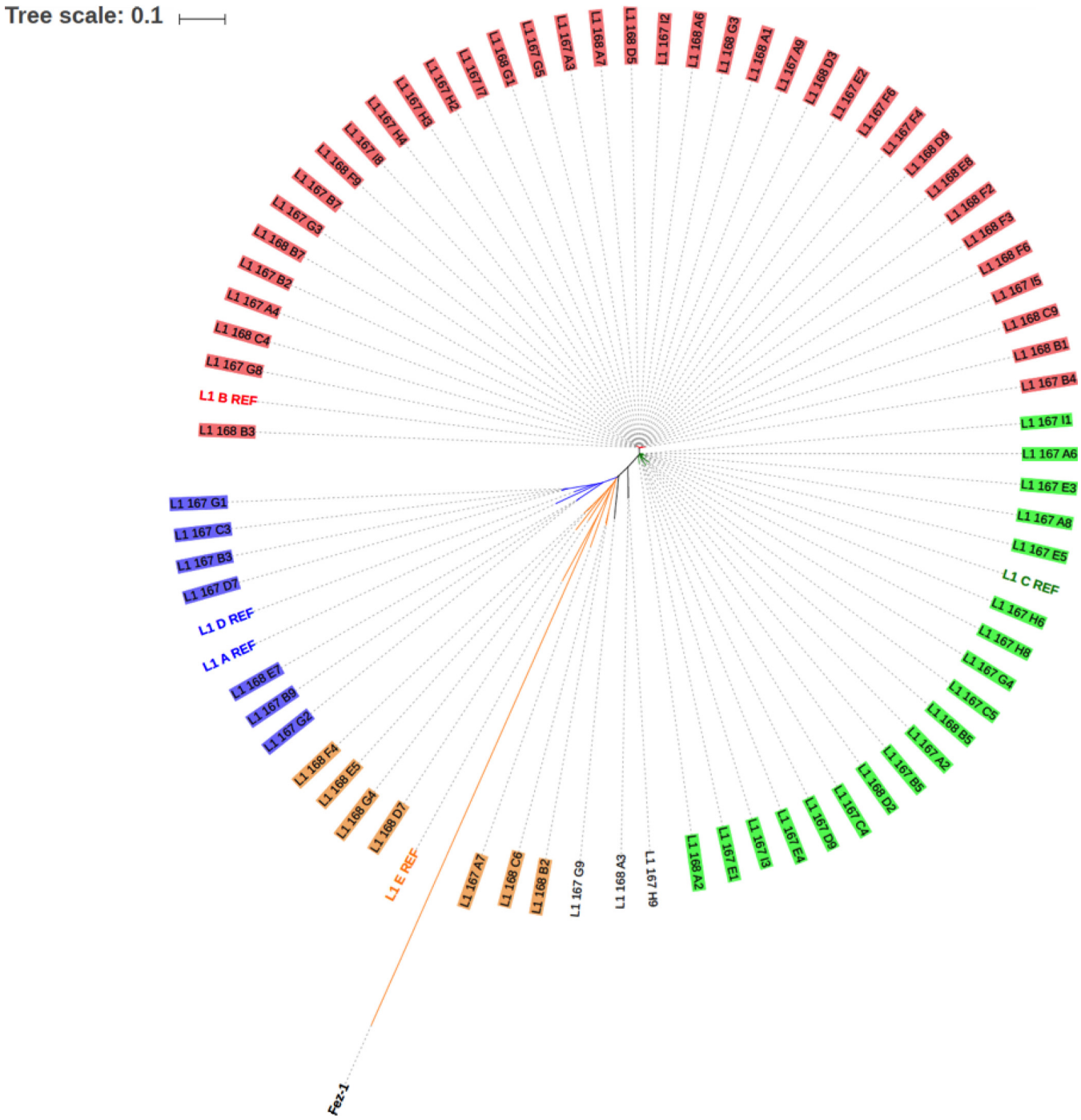

FIG 3 Unrooted circular cladogram of clinical L1 sequences. bla_{L1} genes from 73 clinical isolates were sequenced, and the inferred amino acid sequences of the mature enzymes (without the leader sequence) were used in the analysis. Sequences of five variants of L1 described by Avison et al. (21) and the FEZ-1 amino acid sequence (as the outgroup) were included. Alignment was generated using Clustal Omega, and a cladogram was obtained using iTOL (https://itol.embl.de). Branch length represents the genetic distance, with the scale bar indicating the number of substitutions per residue. Clades are highlighted by different colors.

(2, 25). A comparison of susceptibility data found in the strains associated with infection in this collection to those previously reported for strains collected in the United States in the last 2 decades shows that the resistance toward TMP-SMX, ciprofloxacin (CIP), TIC-CLV, and ceftazidime (CAZ) is increasing (2, 27, 28, 29). For instance, the percentage of strains susceptible to TMP-SMX in 1997 to 1999 was 95%; in 2001, it was 90.5%; in 2003 to 2008, it went up again to 97%; and in our collection, it ranged from 79% to 96%,

Downloaded from http://mbio.asm.org/ on April 15, 2021 by guest

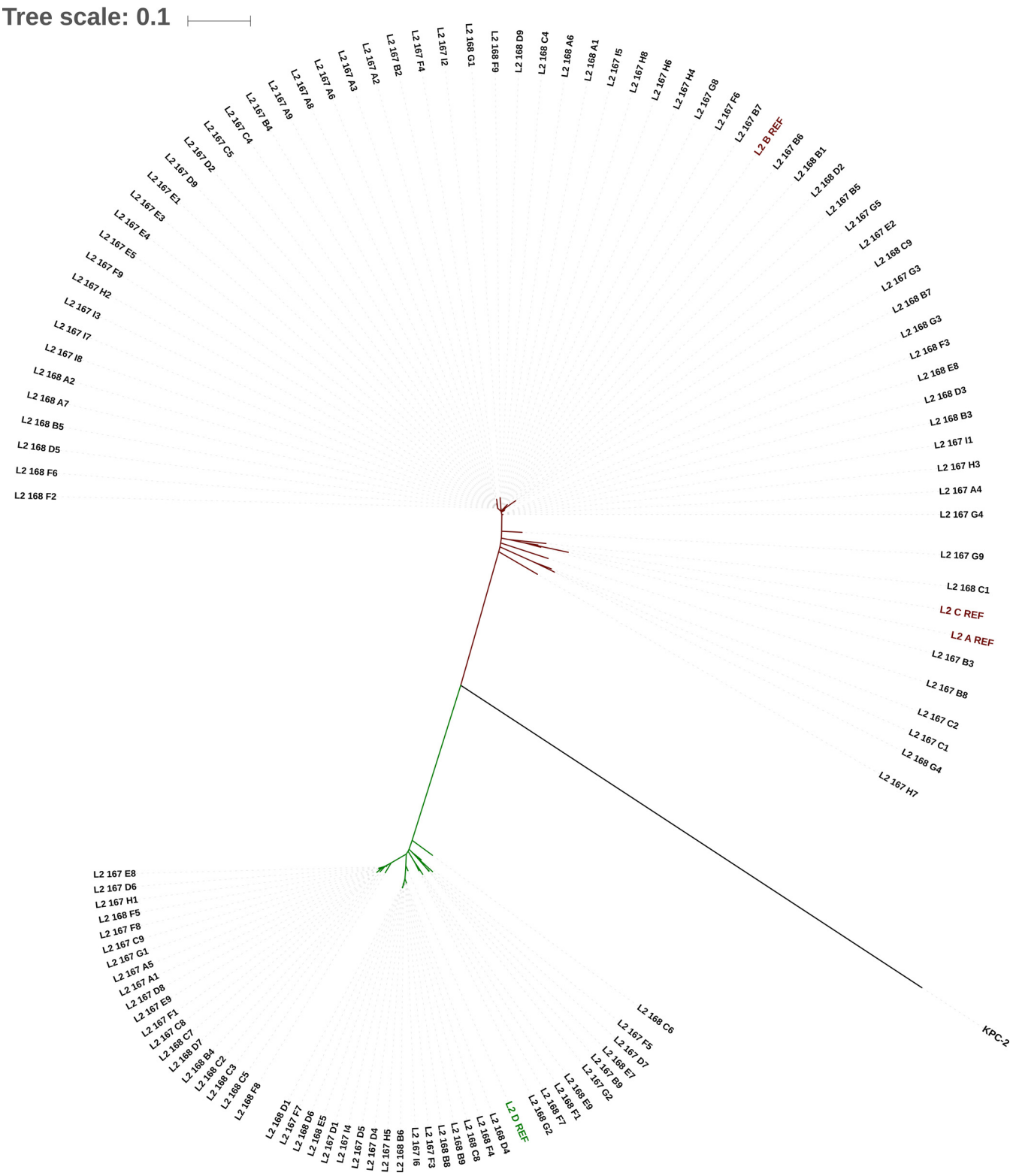

FIG 4 Unrooted circular cladogram of clinical L2 sequences. bla_{L2} genes from 115 clinical isolates were sequenced, and the inferred amino acid sequences of the mature enzymes (without the leader sequence) were used in the analysis. Sequences of four variants of L2 described by Avison et al. (21) and the KPC-2 amino acid sequence (as the outgroup) were included. Alignment was generated using Clustal Omega, and a cladogram was obtained using iTOL (https://itol.embl.de). Branch length represents the genetic distance, with the scale bar indicating the number of substitutions per residue. Clades are highlighted by different colors.

Downloaded from http://mbio.asm.org/ on April 15, 2021 by guest

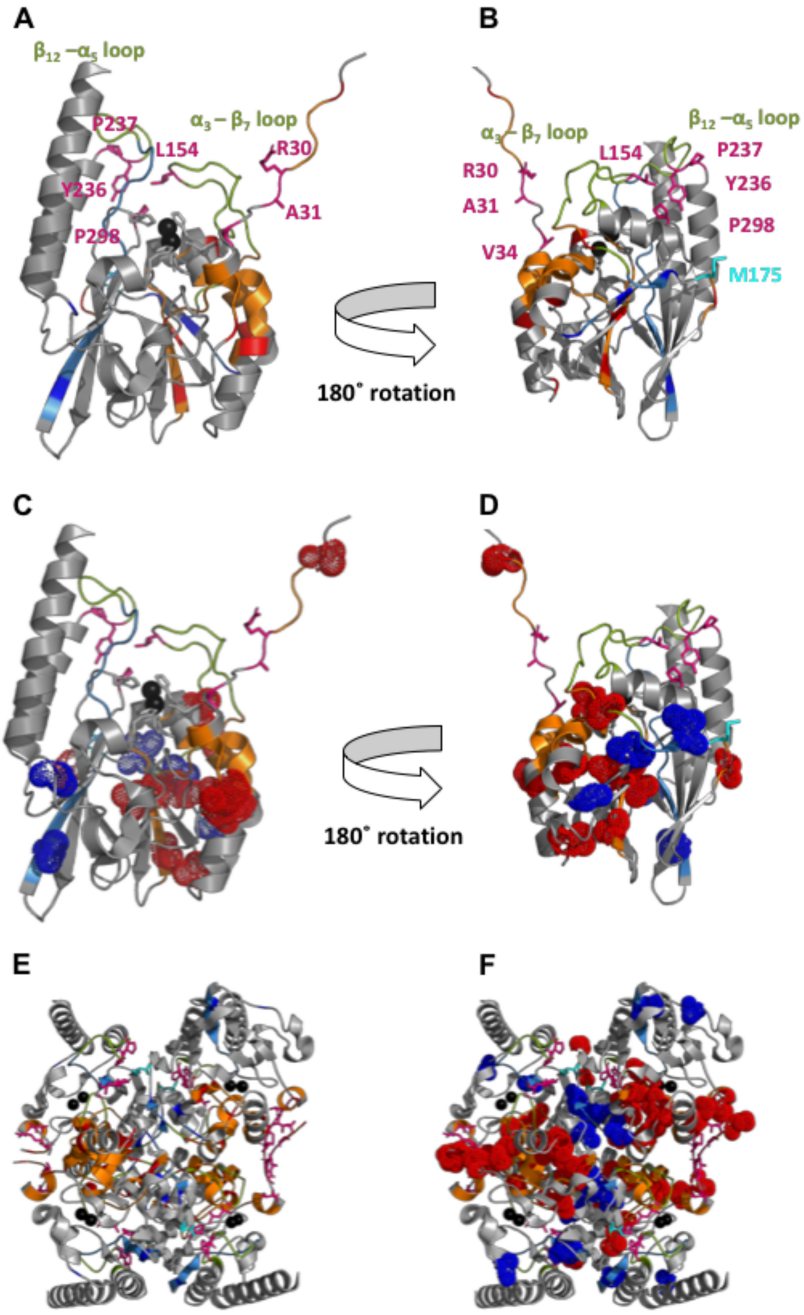

FIG 5 PyMOL visualization of two clusters of covarying residues obtained using the BIS2Analyzer on the L1 MBL monomer (A to D) and tetramer (E and F). Clusters 2 and 4 are highlighted in orange and blue, respectively, on the L1 MBL monomer (PDB ID 2AIO) and tetramer (PDB ID 2QIN) structures. True covarying residues are displayed in darker colors (red and dark blue), whereas residues affected by that covariance are represented in orange and a lighter shade of blue. In panels A, B, and E, clusters are shown as ribbons, whereas in panels C, D, and F, the covarying residues only are represented as dots. Panels B and D show the clusters from a different perspective, after a 180° turn. In all sets, important residues are displayed as sticks, gray for the Zn-binding residues, cyan for Met175, the main residue involved in tetramerization, and magenta for some other secondary interaction within the tetramer. Zn(II) ions are represented as black spheres, and active-site loops are shown in green.

being lower in the isolates collected from blood, likely reflecting collection after treatment of the patient with antibiotics, including TMP-SMX. Similarly, the susceptibility reported for CIP in 1997 to 1999 was 55%; in 2001, it was 52%; and in this study, it was 25% to 38%, the lowest corresponding to isolates from the bloodstream infections. The situation is more dramatic for the β-lactams: the susceptibility to

Downloaded from http://mbio.asm.org/ on April 15, 2021 by guest

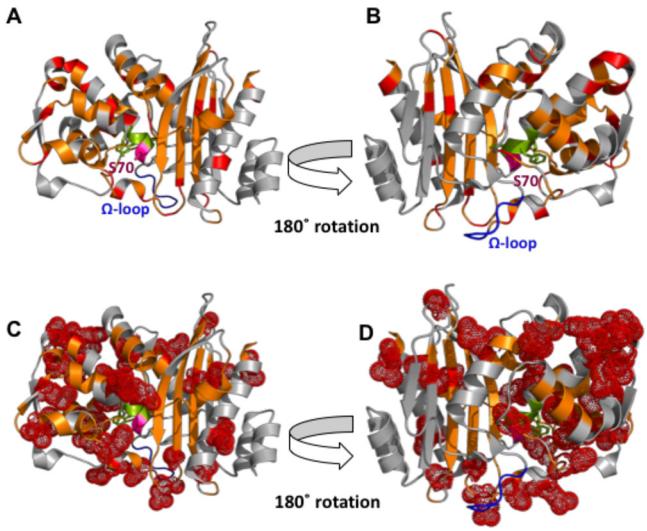

FIG 6 PyMOL visualization of the cluster of covarying residues identified by BIS2Analyzer on the L2 serine β-lactamase (PDB ID 1N4O). (A and B) Covarying residues are displayed in red, whereas orange represents residues affected by that covariance. (C and D) Covarying residues only are shown as dots in the surface representation. Catalytically important residues (located in the SDN loop) are displayed as green sticks, while S70 is highlighted in magenta sticks. Residues of the Ω-loop, not included in the cluster, are shown in blue.

TIC-CLV reported in 1997 to 1999 was 90%; in 2001, it was 48%; in 2003 to 2008, it was 46%; and herein we report a susceptibility of 18% to 25%. For CAZ, the susceptibility reported in 1997 to 1999 was 67%; in 2003 to 2008, it was 51%; and in this study, it ranged from 16% to 43%, being the lowest for isolates collected from CF patients (2, 27–29). A downward trend of susceptibility to antimicrobial agents and an upswing in the frequency of isolates with multidrug resistance were also recently found in a study conducted in China on 300 *S. maltophilia* strains collected over a 10-year period (16). In that study, however, the percentage of strains susceptible to minocycline (MIN) was found to be also decreasing, whereas our data show outstanding rates of susceptibility to this tetracycline.

Importantly, we also show excellent susceptibility rates for the novel combination ceftazidime-avibactam and aztreonam (CZA-ATM), especially when the aztreonam is used at 8 mg/liter. Remarkably, we demonstrate that the susceptibility to CZA-ATM of the strains recovered from blood and from other infections (most of them respiratory samples) is higher than the susceptibility to TMP-SMX, which is the "first-line" antibiotic to treat *S. maltophilia* infections. The activity of CZA-ATM toward the strains recovered from patients with CF is comparable to the activity of TMP-SMX. Therefore, these results confirm previous findings regarding the *in vivo* and *in vitro* efficacy of CZA-ATM against *S. maltophilia* (13, 14). Further observational and controlled studies are planned to add clinical data on the utility and safety of CZA-ATM therapy.

Previous genotyping studies showed that *S. maltophilia* is a highly heterogeneous species (18, 30). The identification of a number of different STs and previously unrecognized allelic combinations demonstrates the high genetic diversity of the study sample. Consequently, specific associations between the genetic background and either the clinical origin, place, or time of collection were not identified. Nevertheless, ST5, previously found to be the predominant ST in France and reported in Germany, Austria, and Korea, was the most common ST in our collection (20, 31, 32). Larger studies should be performed to confirm the putative success of this genetic background, since only 6 of 83 strains were ST5 in the French study and 9 of 130 representatives of this ST were identified in the present study.

The initial genomic characterization of *S. maltophilia* by Hauben et al. (18) using amplified fragment length polymorphism (AFLP) suggested an association between

Downloaded from http://mbio.asm.org/ on April 15, 2021 by guest

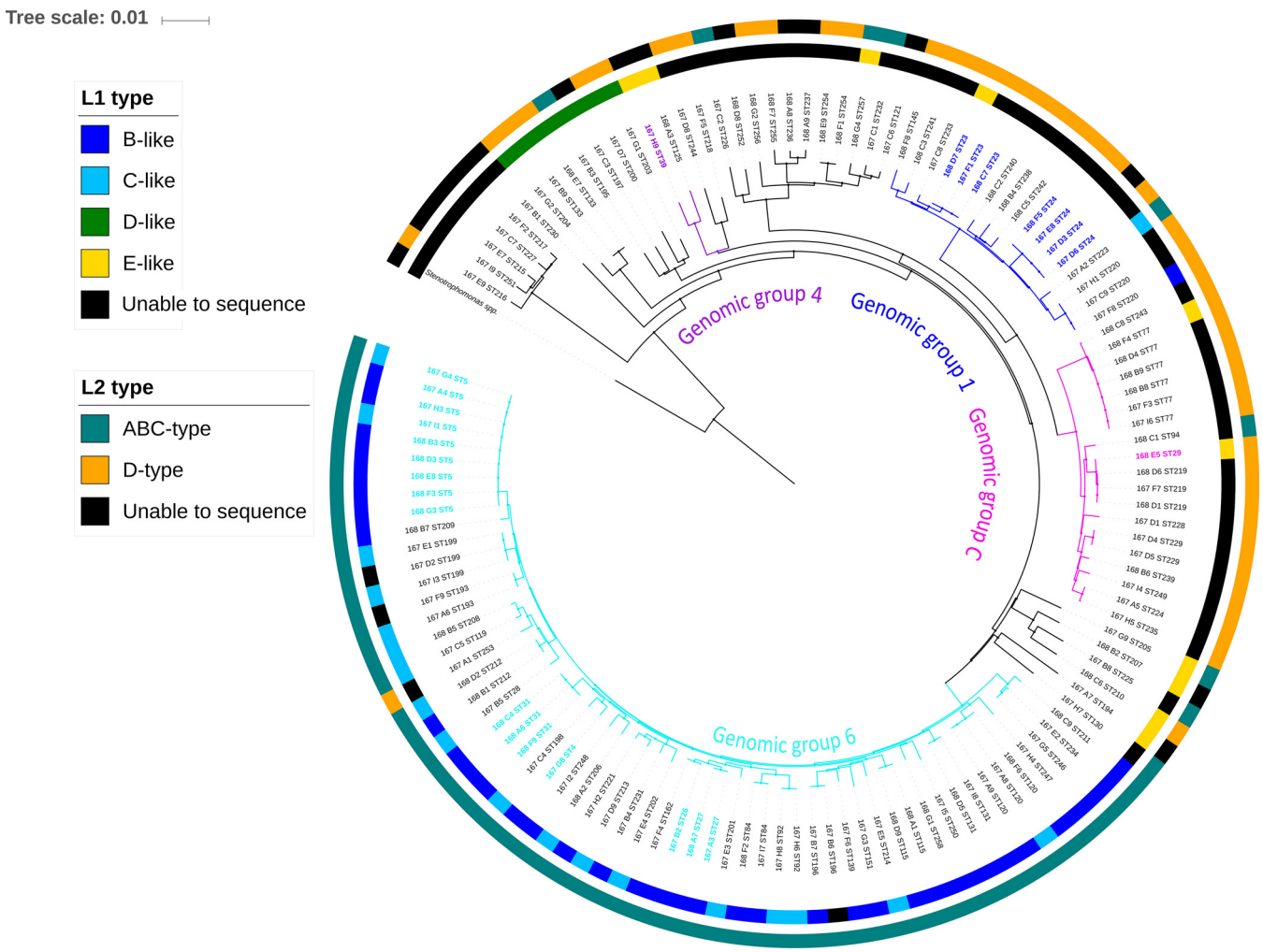

FIG 7 Putative association of specific types of L1 and L2 -lactamases with genomic group 6. Phylogenetic analysis of *S. maltophilia* from concatenated sequences of the seven housekeeping gene fragments (3,591 nt). A consensus UPGMA tree shows the structure of the studied *S. maltophilia* population ($n = 130$). Branch length represents the genetic distance, with the scale bar indicating the number of substitutions per nucleotide position. The tree was rooted with a sequence from *Stenotrophomonas* spp. (not *S. maltophilia*). The genomic group designation according to MLST in the original study by Kaiser et al. (20) is indicated by colored branches: cyan, genomic group 6; blue, genomic group 1; purple, genomic group 4; magenta, genomic group C. Known STs belonging to each genomic group are highlighted in their corresponding color. Internal and external rings indicate L1 and L2 types, respectively.

some genomic groups and environmental or human sources (19). In that study, some genomic groups contained exclusively environmental strains (4, 9, and 10), whereas others, such as genomic groups 1, 6, and 7, included mostly clinical isolates (18). These findings were not only confirmed but also expanded by the MLST scheme proposed by Kaiser et al. (20). Since then, several other studies employed the genomic group determination based on the concatenation and alignment of the sequences corresponding to the seven housekeeping genes included in the *S. maltophilia* MLST scheme as an efficient approach to study the population structure of this pathogen (32–34). In line with other studies, we also report the predominance of genomic groups 6, 1, and C among our clinical samples, all of which have previously been associated with human sources (20, 31). Moreover, our results show a putative association of genomic group 6 with B-like and C-like type L1 enzymes and ABC-like type L2 variants (Fig. 7).

The apparent emergence of strains with unique genetic backgrounds associated with human pathogenicity may indicate an ongoing process by which *S. maltophilia* adapts to this specific niche. Such adaptation processes might be driven by conditions

Downloaded from http://mbio.asm.org/ on April 15, 2021 by guest

in the hospital environment that could promote survival of certain strains with new genomic and phenotypic characteristics.

A closer look into the β-lactamase-encoding genes reveals their molecular heterogeneity. Among the 130 strains included, we identified 34 novel allelic variants of bla_{L1} and 43 of bla_{L2}. In both cases, variable residues are scattered throughout the protein. As observed in all cases of MBL allelic variants, the identity of key residues is preserved, such as the metal ligands in L1 (His116, His118, and His196, which coordinate Zn1, and Asp120, His121, and His263, which coordinate Zn2), which are fully conserved. The active site of L1 MBL is completed by the second-shell residues, which maintain the orientation of the Zn-binding residues through an extensive hydrogen-bonding network, in addition to hydrophobic interactions (35). Residues involved in the H-bonding network include Asp68, Asp84, Asp153, and Ser221. Interestingly, our MSA identified Asp68 as one of the most variable residues in L1; in fact, substitutions for Asp68 were found in 7 out of the 73 L1 sequences, being replaced by Asn, Gly, and Ser residues, i.e., the three smallest and most flexible amino acids (see Table S1 in the supplemental material). Studies of the second-shell residues Ser84 and Gly121 in SPM-1 (36) and Ser262 in IMP-1 (37, 38) B1 MBLs have demonstrated that these residues can modulate substrate preference. Considering that substitutions which tune flexibility result in modulation of the substrate spectrum in the related MBL from *Bacillus cereus* (39), we hypothesize that Asp68 substitutions in L1 could potentially result in subtle changes in the substrate preference.

The metal center of L1 is surrounded by two protruding loops, α3-β7 and β12-α5. The α3-β7 loop comprises 22 residues (Arg148 to Arg172) and extends over the active site. Residues located at this flexible loop are thought to make hydrophobic interactions with large hydrophobic motifs at C-2 or C-6 of the β-lactam substrates and consequently determine the enzyme's substrate spectrum (35, 40, 41, 42). On the other hand, the β12-α5 loop includes 20 residues (Arg219 to Leu240) and sits adjacent to the active site. From this loop, two important residues project into the active site and serve as an indirect ligand of Zn2 (Ser221) and as a second-shell residue of His196 (Ser223) (35). In our set of 73 clinical isolates, 3 isolates were found carrying two novel substitutions at the α3-β7 loop: Gly158Ala and (Gly/Glu)161Asp. Gly158 is located at the tip of the loop, next to Phe157, whose role in substrate binding and catalysis has been evidenced by molecular modeling, crystal structures of L1 in complex with ligands, directed mutagenesis, and kinetic studies (35, 40–42). The Gly158Ala substitution could disturb the positioning of Phe157 by restricting the flexibility of the peptide chain. Likewise, the Gly161Asp substitution could alter the enzyme's catalytic efficiency, as is the case for Gly161Glu, which decreases the overall performance of the L1 E variant toward nitrocefin and imipenem, compared with that of the L1 A variant (21). Notably, substitutions at this residue are found in isolates that cluster together with the L1 E variant (Fig. 3 and Table S1).

Five isolates carried novel substitutions in the β12-α5 loop: Gln230Arg, Gly233Asp, (Lys/Gln)232Arg, and (Pro/Ala)235Val. Although none of these residues has been shown to directly interact with the substrate, catalytically important residues like Ser221 and Ser223 protrude into the active site from this loop. Ser221 coordinates the Zn2-bound apical water, whereas Ser223 directly interacts with the substrate C_4 carboxylate group (42). Consequently, substitutions that lead to changes in the overall conformation of this loop, either by strengthening or weakening the H-bonding network that maintains it in place or by changing its electrostatic characteristics, could ultimately affect substrate catalysis.

L1 is an unusual β-lactamase, since it is biologically functional as a homotetramer (24, 35). The crystal structure of the L1 enzyme submitted under PDB ID 2QIN shows that the tetramer is formed by three main sets of intramolecular interactions that result in each subunit making contact with each of the other three (35) (Fig. S6). First, there are hydrophobic interactions and hydrogen bonds between residues located in the extended N terminus. Second, Leu26 and Leu29 from subunit B (and D) dock in hydrophobic pockets formed by Ala31 and Tyr32 and by Met87, Pro89,

Downloaded from http://mbio.asm.org/ on April 15, 2021 by guest

Gln90, Met91, and His94 of subunit A (and C), respectively. Remarkably, none of our clinical strains demonstrate any variation affecting these interactions. In fact, only the L1 E variant possesses a His94Tyr substitution. In the third and most important intramolecular interaction, the side chain of Met175 from subunit C (and B) penetrates a hydrophobic pocket formed by several residues in subunit A (and D), including Pro237, Tyr236, Leu154, and Pro198. The importance of Met175 in the tetramer formation was demonstrated by Simm et al., when their Met175Asp variant produced only monomeric L1 (24). Conservation of these residues among all clinical samples and the five L1 references indicates that tetramerization is fundamental for the function of this enzyme.

A minor set of interactions maintain contact between subunits A and D and between subunits B and C of the homotetramer. In this, Lys135 in subunit A (and B) form hydrogen bonds with Lys129, Thr132, and Ala134 in subunit D (and C). Likewise, Arg107 in subunit A (and B) form hydrogen bonds with Asp78 in subunit D (and C). In contrast to what was observed for the main interactions, sequence variability was found at positions 129, 135, and 132 in the clinical isolates. In fact, the identity of residues at position 135 is quite variable, as it can be a Glu, His, Lys, Arg, Met, or Ser. In the other cases, only one substitution was found (Lys129Met or Thr132Ser). Given that this set of interactions plays a minor role, it is unlikely to affect tetramerization.

In contrast to the L1 β-lactamase, sequences of the L2 β-lactamase were of two distinct types, sharing approximately 70% homology. Of the 116 L2 sequences obtained, 67 (59%) belonged to type ABC and 47 (41%) belonged to type D. As expected, we did not find mutations in the highly conserved structural motifs of class A β-lactamases: the active-site pocket Ser70-X-X-Lys73, the SDN loop Ser130-Asp131-Asn132, and Lys234-Thr(Ser)235-Gly236. Within the SDN loop, Ser130 is part of a critical proton shuttle during both the acylation and deacylation of β-lactams (43–45). Furthermore, the SDN loop is associated with maintaining the structure of the active-site cavity, enzyme stability, and stabilization of the enzyme transition state (43). As a result, the alpha-helixes before and after this motif are expected to be highly conserved. However, we found two L2 variants (three total sequences) containing the mutations Thr126Ala and Thr129Ile, just preceding the SDN loop. The hydroxyl side chain of both threonine residues interacts directly with Asp131 (of SDN) in the L2 crystal structure (PDB ID 1N4O). Loss of this interaction could directly affect the catalytic mechanisms of these enzymes by changing the structure of the active-site pocket, including the positioning of Ser130.

Another important structural element of serine β-lactamases is the Ω-loop, which encompasses residues 164 to 179 and constitutes the "back wall" or "floor" of the active site that shapes the binding cavity (46). As expected, important residues within this loop, like Arg164, Glu166, and Asp179, were conserved among all the L2 variants. However, as shown in Fig. S4B, we found a significant number of substitutions in this region, including Leu165Asn and Ser171Leu. In the L2 enzyme submitted under PDB ID 1NO4, Leu165 forms a small hydrophobic cluster underneath the polar surface, together with Phe139, Pro145, and Leu169. However, the slightly exposed position of residue 165 would perfectly allow for a polar amide side chain of an Asn to come into contact with the surrounding solvent and possibly form an H bond with Asn136. On the other hand, the OH group of Ser171 snorkels out to the surface and is surrounded by three pockets with crystallographic water. Substitution by Leu could be relaxed by displacing water molecules from one of these cavities to locate the longer, hydrophobic side chain. Since the Ω-loop plays a crucial role in substrate recognition and catalysis, amino acid substitutions in this loop are associated with the expansion of the β-lactamase substrate spectrum (47–49). The study of the effect of these novel substitutions on the catalytic activity and inhibitor binding to L2 is warranted (Fig. S7).

Finally, the Leu103Gln substitution was observed in a single sequence. The change from a hydrophobic to a polar side chain could have an impact, especially since this amino acid resides on the loop located at the entrance of the active site (residues

Downloaded from http://mbio.asm.org/ on April 15, 2021 by guest

102-110), alongside the critical His105, which forms direct interactions with β-lactam substrates. An amino acid substitution at position 103 could alter the position of this loop, as well as the orientation of residue 105 (50–52). The remaining nonconservative substitutions occurred almost exclusively in catalytically unimportant regions on the periphery of the enzyme, including the N and C termini and the solvent-exposed regions. The effect of these substitutions is yet to be determined.

Conclusions. In this work, we explored the microbiological characteristics, population structure, and sequence diversity of the β-lactamase-encoding genes in clinical isolates of *S. maltophilia*. Overall, our results raise the concern of an increasing trend in resistance toward traditional antibiotics, such as TMP-SMX, and highlight the excellent *in vitro* performance of the novel combination CZA-ATM against this pathogen. Our data also confirm the predominance of genomic group 6 among strains responsible for hospital-associated infections. The putative association of this genomic group with specific variants of L1 and L2 points to an adaptation of *S. maltophilia* to human pathogenicity and warrants further studies aimed at determining the biochemical characteristics of these enzymes. Second-shell mutations in MBLs and mutations in the Ω-loop of class A enzymes have been shown to affect substrate and inhibitor binding. Therefore, the allelic variations should be taken into account for the design of effective inhibitors and the preservation of current antibiotics.

MATERIALS AND METHODS

Ethics statement. Ethics approval was not required for this study. *S. maltophilia* strains were obtained from an archived library of *S. maltophilia* clinical samples at the Louis Stokes Cleveland Veterans Affairs Medical Center, collected between 2006 to 2016 from collaborating centers across the United States (University Hospitals, Cleveland, OH; Nationwide Children's Hospital, Columbus, OH; New York Presbyterian Hospital/New York-Presbyterian/Weill Cornell Medical Center, New York, NY; Duke University, Durham, NC; Johns Hopkins Hospital, Baltimore, MD; University of Washington, Seattle, WA; and the *Burkholderia cepacia* Research Laboratory and Repository at the University of Michigan, Ann Arbor, MI). All samples were anonymized and assigned internal identification codes. Basic anonymized metadata were obtained for analysis, including date and location of collection, cystic fibrosis status, and clinical specimen origin. The collection of 130 strains includes two strains recovered from abiotic surfaces of a hospital and *S. maltophilia* ATCC 33551 (internal code 167_A1).

Strain identification. Identification as *S. maltophilia* was based on conventional techniques, automated instruments, including Vitek-2 (bioMérieux, Marcy-l'Etoile, France), and mass spectrometry (Microflex; Bruker Corporation, Billerica, MA). Isolates were plated on Trypticase soy agar II with 5% sheep blood (Becton, Dickinson GmbH, Heidelberg, Germany) to confirm their purity.

Susceptibility assays. MICs were determined by agar dilution methods according to the guidelines of the Clinical and Laboratory Standards Institute (CLSI) (26). The following antibiotics/inhibitors were included: trimethoprim-sulfamethoxazole (TMP-SMX; Sigma, St. Louis, MO), ciprofloxacin (CIP; Fluka, Buchs, Switzerland), minocycline (MIN; Sigma, St. Louis, MO), ticarcillin-clavulanate (TIC-CLV; Sigma, St. Louis, MO), ceftazidime (CAZ; Sigma, St. Louis, MO), aztreonam (ATM; Bristol-Myers Squibb, New York, NY), and ceftazidime-avibactam (CZA) and ceftazidime-avibactam and aztreonam (CZA-ATM) combinations using the avibactam-free acid at a constant concentration of 4 g/liter from Advanced ChemBlock, Inc. (Burlingame, CA). *Escherichia coli* ATCC 25922 and ATCC 35218 were included as quality controls. Where breakpoints for *S. maltophilia* were not available, those for *Pseudomonas aeruginosa* were used, as has been previously done (13).

MLST. Total DNA was extracted using the UltraClean microbial DNA isolation kit (MoBio Laboratories, Carlsbad, CA) and used as the template to amplify and sequence seven housekeeping genes of *S. maltophilia*, namely *atpD*, *gapA*, *guaA*, *mutM*, *nuoD*, *ppsA*, and *recA*, according to the protocol proposed by Kaiser et al. (20) and the *S. maltophilia* multilocus sequence typing (MLST) database available at http://pubmlst.org/smaltophilia/. Clonal analysis was performed using eBURST v3 (http://eburst.mlst.net). Additional genetic relatedness was estimated based on alignments of the concatemers of the seven allelic sequences of the seven housekeeping genes (final length, 3,591 nucleotides [nt]) generated using Clustal Omega and obtained using iTOL (https://itol.embl.de), using branch length, and rooted on corresponding *Stenotrophomonas* spp. (not *S. maltophilia*) sequences. Genomic groups were assigned based on the initial classification by Hauben et al. and expanded by Kaiser et al. (18, 20).

Chromosomal β-lactamase detection and sequencing. Previously published primers L1 Full Fdw (5′-ACC ATG CGT TCT ACC CTG CTC GCC TTC GCC-3′) and L1 Full Rev (5′-TCA GCG GGC CCC GGC CGT TTC CTT GGC CAG-3′) and L2 Full Fdw (5′-CGATTCCTGCAGTTCAGT-3′) and L2 Full Rev (5′-CGGTTACCT CATCCGATC-3′) were used to sequence the complete open reading frames (ORFs) of bla_{L1} and bla_{L2}, respectively (21). Amplicons were sequenced at Molecular Cloning Laboratories (MCLAB; San Francisco, CA). In cases where the reaction with these primers failed, detection of the *bla* genes was performed by using alternative primers designed to amplify an internal region of 218 pb of bla_{L1} (SmaI_L1_F, 5′-ATC ATC ATG GAT GGC GAA GT-3′; SmaI_L1_R, 5′-AAG CTG CGC TTG TAG TCC TC-3′) and 783 pb of an intergenic region between the regulator AmpR and the bla_{L2} gene (SmaI_AmpR_L2_F, 5′-CGG GAG ACG

Downloaded from http://mbio.asm.org/ on April 15, 2021 by guest

ATG GAA CAG-3′; Smal_AmpR_L2_R, 5′-GTG TTG TCG CTG GTG ATG A-3′). For 9 isolates, the sequences of L1 and L2 were extracted from the *Stenotrophomonas* whole-genome sequences available in GenBank (BioProject no. PRJNA390523).

Sequence analysis. DNA and deduced protein sequences were analyzed by using the Lasergene Molecular Biology Suite software (DNASTAR, Inc., Madison, WI). Mature protein sequences were obtained after identification and removal of the signal peptide by using standard parameters on the SignalP 4.1 server (http://www.cbs.dtu.dk/services/SignalP/). The protein sequence logo was generated at the host server of the University of California at Berkeley (http://weblogo.berkeley.edu/logo.cgi). The amino acid sequence of mature proteins was aligned using the Clustal Omega algorithm against L1 and L2 reference variants (21), and unique substitutions were identified. Protein dendrograms were plotted using iTOL (https://itol.embl.de/), based on the guide tree constructed by Clustal Omega using the unweighted pair group method using average linkages (UPGMA method). Discovery Studio (Dassault Systèmes BIOVIA, Discovery Studio Modeling Environment, release 2017, San Diego, CA; Dassault Systèmes, 2016) software was used to map unique substitutions onto the crystal structure of the L1 monomer (PDB ID 2AIO), the L1 tetramer (PDB ID 2QIN), and L2 (PDB ID 1N4O). Inspection of site-specific amino acid variability was guided by analysis using the PsychoProt server (53, 54).

Covariance analysis. Amino acid sequences of the detected novel L1 and L2 variants plus the references previously described by Avison et al. (21) were aligned using the Clustal Omega algorithm. Alignment was then submitted to the BIS2analyzer website, which is tailored for data sets of high conservation (http://www.lcqb.upmc.fr/BIS2Analyzer/submit.php#) (55), and using the NJ algorithm, clusters of covarying amino acid residues were identified. Clusters were then mapped onto the crystal structure of the L1 monomer (PDB ID 2AIO), the L1 tetramer (PDB ID 2QIN), and L2 (PDB ID 1N4O).

Accession number(s). The nucleotide sequences of the new bla_{L1} and bla_{L2} alleles are available under NCBI reference sequence accession numbers MK871676 to MK871737 and MK888855 to MK888979, respectively.

SUPPLEMENTAL MATERIAL

Supplemental material for this article may be found at https://doi.org/10.1128/mBio.00405-19.

FIG S1, EPS file, 1.8 MB.
FIG S2, TIF file, 0.6 MB.
FIG S3, JPG file, 0.04 MB.
FIG S4, TIF file, 1.7 MB.
FIG S5, TIF file, 0.5 MB.
FIG S6, TIF file, 0.8 MB.
FIG S7, TIF file, 0.3 MB.
TABLE S1, PDF file, 0.1 MB.
TABLE S2, PDF file, 0.1 MB.
DATASET S1, XLSX file, 0.1 MB.

ACKNOWLEDGMENTS

M.F.M. was the recipient of a doctoral scholarship from Colciencias. A.J.V. is a staff member from CONICET. Research reported in this publication was supported in part by grants from the National Institute of Allergy and Infectious Diseases of the National Institutes of Health under award numbers R01AI100560, R01AI063517, R21AI114508, and R01AI072219 to R.A.B. and U19AI110819 to D.E.F. This study was supported in part by funds and/or facilities provided by the Cleveland Department of Veterans Affairs, award number 1I01BX001974, from the Biomedical Laboratory Research & Development Service of the VA Office of Research and Development and the Geriatric Research Education and Clinical Center VISN 10 to R.A.B.

The content is solely the responsibility of the authors and does not necessarily represent the official views of the National Institutes of Health or the Department of Veterans Affairs.

M.F.M. and J.D.R. performed the microbiological and molecular analysis. M.F.M. and M.T. constructed the molecular models of proteins. M.F.M. and L.A.A. performed the covariance analysis. D.E.F. obtained whole-genome sequences. M.F.M., J.D.R., M.T., and K.M.P.-W. analyzed and discussed the protein variability data. J.J.L. and T.J.W. provided some strains and helped with the analysis of the microbiological data. T.J.W., A.J.V., and R.A.B. conceived the study. M.F.M., K.M.P.-W., L.A.A., A.J.V., and R.A.B. analyzed and discussed the data and wrote the paper, and all authors discussed the results and commented on the manuscript.

Downloaded from http://mbio.asm.org/ on April 15, 2021 by guest

REFERENCES

1. Brooke JS. 2012. *Stenotrophomonas maltophilia*: an emerging global opportunistic pathogen. Clin Microbiol Rev 25:2–41. https://doi.org/10.1128/CMR.00019-11.
2. Chang Y-T, Lin C-Y, Chen Y-H, Hsueh P-R. 2015. Update on infections caused by *Stenotrophomonas maltophilia* with particular attention to resistance mechanisms and therapeutic options. Front Microbiol 6:893. https://doi.org/10.3389/fmicb.2015.00893.
3. Falagas ME, Kastoris AC, Vouloumanou EK, Dimopoulos G. 2009. Community-acquired *Stenotrophomonas maltophilia* infections: a systematic review. Eur J Clin Microbiol Infect Dis 28:719–730. https://doi.org/10.1007/s10096-009-0709-5.
4. Looney WJ, Narita M, Mühlemann K. 2009. *Stenotrophomonas maltophilia*: an emerging opportunist human pathogen. Lancet Infect Dis 9:312–323. https://doi.org/10.1016/S1473-3099(09)70083-0.
5. Adegoke AA, Stenström TA, Okoh AI. 2017. *Stenotrophomonas maltophilia* as an emerging ubiquitous pathogen: looking beyond contemporary antibiotic therapy. Front Microbiol 8:2276. https://doi.org/10.3389/fmicb.2017.02276.
6. Cho SY, Lee DG, Choi SM, Park C, Chun HS, Park YJ, et al. 2015. *Stenotrophomonas maltophilia* bloodstream infection in patients with hematologic malignancies: a retrospective study and in vitro activities of antimicrobial combinations. BMC Infect Dis 15:1–8. https://doi.org/10.1186/s12879-015-0801-7.
7. Friedman ND, Korman TM, Fairley CK, Franklin JC, Spelman DW. 2002. Bacteraemia due to *Stenotrophomonas maltophilia*: an analysis of 45 episodes. J Infect 45:47–53. https://doi.org/10.1053/jinf.2002.0978.
8. Micozzi A, Venditti M, Monaco M, Friedrich A, Taglietti F, Santilli S, Martino P. 2000. Bacteremia due to Stenotrophomonas maltophilia in patients with hematologic malignancies. Clin Infect Dis 31:705–711. https://doi.org/10.1086/314043.
9. Brooke JS, Di Bonaventura G, Berg G, Martinez J-L. 2017. Editorial: A multidisciplinary look at *Stenotrophomonas maltophilia*: an emerging multi-drug-resistant global opportunistic pathogen. Front Microbiol 8:1511. https://doi.org/10.3389/fmicb.2017.01511.
10. World Health Organization. 2018. Public health importance of antimicrobial resistance. https://www.who.int/drugresistance/AMR_Importance/en/.
11. Crossman LC, Gould VC, Dow JM, Vernikos GS, Okazaki A, Sebaihia M, Saunders D, Arrowsmith C, Carver T, Peters N, Adlem E, Herhornou A, Lord A, Murphy L, Seeger K, Squares R, Rutter S, Quail MA, Rajandream MA, Harris D, Churcher C, Bentley SD, Parkhill J, Thomson NR, Avison MB. 2008. The complete genome, comparative and functional analysis of *Stenotrophomonas maltophilia* reveals an organism heavily shielded by drug resistance determinants. Genome Biol 9:R74. https://doi.org/10.1186/gb-2008-9-4-r74.
12. Okazaki A, Avison MB. 2008. Induction of L1 and L2 β-lactamase production in *Stenotrophomonas maltophilia* is dependent on an AmpR-type regulator. Antimicrob Agents Chemother 52:1525–1528. https://doi.org/10.1128/AAC.01485-07.
13. Mojica MF, Papp-Wallace KM, Taracila MA, Barnes MD, Rutter JD, Jacobs MR, LiPuma JJ, Walsh TJ, Vila AJ, Bonomo RA. 2017. Avibactam restores the susceptibility of aztreonam against clinical isolates of *Stenotrophomonas maltophilia*. Antimicrob Agents Chemother 61:e00777-17. https://doi.org/10.1128/AAC.00777-17.
14. Mojica MF, Ouellette CP, Leber A, Becknell MB, Ardura MI, Perez F, Shimamura M, Bonomo RA, Aitken SL, Shelburne SA. 2016. Successful treatment of bloodstream infection due to metallo-beta- lactamase-producing *Stenotrophomonas maltophilia* in a renal transplant patient. Antimicrob Agents Chemother 60:5130–5134. https://doi.org/10.1128/AAC.00264-16.
15. Alqahtani JM. 2017. Emergence of *Stenotrophomonas maltophilia* nosocomial isolates in a Saudi children's hospital: risk factors and clinical characteristics. Saudi Med J 38:521–527. https://doi.org/10.15537/smj.2017.5.16375.
16. Hu L-F, Xu X-H, Li H-R, Gao L-P, Chen X, Sun N, Liu Y-Y, Ying H-F, Li J-B. 2018. Surveillance of antimicrobial susceptibility patterns among *Stenotrophomonas maltophilia* isolated in China during the 10-year period of 2005–2014. J Chemother 30:25–30. https://doi.org/10.1080/1120009X.2017.1378834.
17. Berg G, Roskot N, Smalla K. 1999. Genotypic and phenotypic relationships between clinical and environmental isolates of *Stenotrophomonas maltophilia*. J Clin Microbiol 37:3594–3600.
18. Hauben L, Vauterin L, Moore ER, Hoste B, Swings J. 1999. Genomic diversity of the genus *Stenotrophomonas*. Int J Syst Bacteriol 49:1749–1760. https://doi.org/10.1099/00207713-49-4-1749.
19. Gherardi G, Creti R, Pompilio A, Di Bonaventura G. 2015. An overview of various typing methods for clinical epidemiology of the emerging pathogen *Stenotrophomonas maltophilia*. Diagn Microbiol Infect Dis 81:219–226. https://doi.org/10.1016/j.diagmicrobio.2014.11.005.
20. Kaiser S, Biehler K, Jonas D. 2009. A *Stenotrophomonas maltophilia* multilocus sequence typing scheme for inferring population structured. J Bacteriol 191:2934–2943. https://doi.org/10.1128/JB.00892-08.
21. Avison MB, Higgins CS, von Heldreich CJ, Bennett PM, Walsh TR. 2001. Plasmid location and molecular heterogeneity of the L1 and L2 β-lactamase genes of *Stenotrophomonas maltophilia* plasmid location and molecular heterogeneity of the L1 and L2 β-lactamase genes of *Stenotrophomonas maltophilia*. Antimicrob Agents Chemother 45:413–419. https://doi.org/10.1128/AAC.45.2.413-419.2001.
22. Jack BR, Meyer AG, Echave J, Wilke CO. 2016. Functional sites induce long-range evolutionary constraints in enzymes. PLoS Biol 14:e1002452. https://doi.org/10.1371/journal.pbio.1002452.
23. Deng Z, Huang W, Bakkalbasi E, Brown NG, Adamski CJ, Rice K, Muzny D, Gibbs RA, Palzkill T. 2012. Deep sequencing of systematic combinatorial libraries reveals β-lactamase sequence constraints at high resolution. J Mol Biol 424:150–167. https://doi.org/10.1016/j.jmb.2012.09.014.
24. Simm AM, Higgins CS, Carenbauer AL, Crowder MW, Bateson JH, Bennett PM, Clarke AR, Halford SE, Walsh TR. 2002. Characterization of monomeric L1 metallo-β-lactamase and the role of the N-terminal extension in negative cooperativity and antibiotic hydrolysis. J Biol Chem 277:24744–24752. https://doi.org/10.1074/jbc.M201524200.
25. El Chakhtoura NG, Saade E, Iovleva A, Yasmin M, Wilson B, Perez F, Bonomo RA. 2018. Therapies for multidrug resistant and extensively drug-resistant non-fermenting gram-negative bacteria causing nosocomial infections: a perilous journey toward 'molecularly targeted' therapy. Expert Rev Anti Infect Ther 16:89–110. https://doi.org/10.1080/14787210.2018.1425139.
26. CLSI. 2018. Performance standards for antimicrobial susceptibility testing: 28th informational supplement M100-S28. Clinical Laboratory and Standards Institute, Wayne, PA.
27. Gales AC, Jones RN, Forward KR, Liñares J, Sader HS, Verhoef J. 2001. Emerging importance of multidrug-resistant *Acinetobacter* species and *Stenotrophomonas maltophilia* as pathogens in seriously ill patients: geographic patterns, epidemiological features, and trends in the SENTRY Antimicrobial Surveillance Program (1997-1998). Clin Infect Dis 32:S104–S113. https://doi.org/10.1086/320183.
28. Flamm RK, Castanheira M, Streit JM, Jones RN. 2016. Minocycline activity tested against *Acinetobacter baumannii* complex, *Stenotrophomonas maltophilia*, and *Burkholderia cepacia* species complex isolates from a global surveillance program (2013). Diagn Microbiol Infect Dis 85:352–355. https://doi.org/10.1016/j.diagmicrobio.2016.03.019.
29. Farrell DJ, Sader HS, Flamm RK, Jones RN. 2014. Ceftolozane/tazobactam activity tested against Gram-negative bacterial isolates from hospitalised patients with pneumonia in US and European medical centres (2012). Int J Antimicrob Agents 43:533–539. https://doi.org/10.1016/j.ijantimicag.2014.01.032.
30. Lira F, Berg G, Martínez JL. 2017. Double-face meets the bacterial world: the opportunistic pathogen *Stenotrophomonas maltophilia*. Front Microbiol 8:2190. https://doi.org/10.3389/fmicb.2017.02190.
31. Kim YJ, Park JH, Seo KH. 2018. Presence of Stenotrophomonas maltophilia exhibiting high genetic similarity to clinical isolates in final effluents of pig farm wastewater treatment plants. Int J Hyg Environ Health 221:300–307. https://doi.org/10.1016/j.ijheh.2017.12.002.
32. Corlouer C, Lamy B, Desroches M, Ramos-Vivas J, Mehiri-Zghal E, Lemenand O, Delarbre J-M, Decousser J-W, Aberanne S, Belmonte O, Blondiaux N, Cattoir V, Dekeyser S, Delarbre JM, Desroches M, Jaouen AC, Laurens E, Lemenand O, Mehiri-Zghal E, Parisi Duchene E, Pangon B, Plassart C, Picot S, Vachee A, Ramos-Vivas J. 2017. *Stenotrophomonas maltophilia* healthcare-associated infections: identification of two main pathogenic genetic backgrounds. J Hosp Infect 96:183–188. https://doi.org/10.1016/j.jhin.2017.02.003.
33. Jayol A, Corlouer C, Haenni M, Darty M, Maillard K, Desroches M, Lamy

Downloaded from http://mbio.asm.org/ on April 15, 2021 by guest

B, Jumas-Bilak E, Madec J-Y, Decousser J-W. 2018. Are animals a source of *Stenotrophomonas maltophilia* in human infections? Contributions of a nationwide molecular study. Eur J Clin Microbiol Infect Dis 37: 1039–1045. https://doi.org/10.1007/s10096-018-3203-0.
34. Madi H, Lukić J, Vasiljević Z, Biočanin M, Kojić M, Jovčić B, Lozo J. 2016. Genotypic and phenotypic characterization of *Stenotrophomonas maltophilia* strains from a pediatric tertiary care hospital in Serbia. PLoS One 11:e0165660. https://doi.org/10.1371/journal.pone.0165660.
35. Ullah JH, Walsh TR, Taylor IA, Emery DC, Verma CS, Gamblin SJ, Spencer J. 1998. The crystal structure of the L1 metallo-beta-lactamase from *Stenotrophomonas maltophilia* at 1.7 A resolution. J Mol Biol 284: 125–136. https://doi.org/10.1006/jmbi.1998.2148.
36. González LJ, Moreno DM, Bonomo RA, Vila AJ. 2014. Host-specific enzyme-substrate interactions in SPM-1 metallo-β-lactamase are modulated by second sphere residues. PLoS Pathog 10:e1003817. https://doi.org/10.1371/journal.ppat.1003817.
37. Oelschlaeger P, Pleiss J. 2007. Hydroxyl groups in the betabeta sandwich of metallo-beta-lactamases favor enzyme activity: Tyr218 and Ser262 pull down the lid. J Mol Biol 366:316–329. https://doi.org/10.1016/j.jmb.2006.11.027.
38. Oelschlaeger P, Schmid RD, Pleiss J. 2003. Modeling domino effects in enzymes: molecular basis of the substrate specificity of the bacterial metallo-β-lactamases IMP-1 and IMP-6. Biochemistry 42:8945–8956. https://doi.org/10.1021/bi0300332.
39. González MM, Abriata LA, Tomatis PE, Vila AJ. 2016. Optimization of conformational dynamics in an epistatic evolutionary trajectory. Mol Biol Evol 33:1768–1776. https://doi.org/10.1093/molbev/msw052.
40. Carenbauer AL, Garrity JD, Periyannan G, Yates RB, Crowder MW. 2002. Probing substrate binding to metallo-β-lactamase L1 from Stenotrophomonas maltophilia by using site-directed mutagenesis. BMC Biochem 3:4. https://doi.org/10.1186/1471-2091-3-4.
41. Nauton L, Kahn R, Garau G, Hernandez JF, Dideberg O. 2008. Structural insights into the design of inhibitors for the L1 metallo-β-lactamase from *Stenotrophomonas maltophilia*. J Mol Biol 375:257–269. https://doi.org/10.1016/j.jmb.2007.10.036.
42. Spencer J, Read J, Sessions RB, Howell S, Blackburn GM, Gamblin SJ. 2005. Antibiotic recognition by binuclear metallo-beta-lactamases revealed by X-ray crystallography. J Am Chem Soc 127:14439–14444. https://doi.org/10.1021/ja0536062.
43. Drawz SM, Bonomo RA. 2010. Three decades of β-lactamase inhibitors. Clin Microbiol Rev 23:160–201. https://doi.org/10.1128/CMR.00037-09.
44. Meroueh SO, Fisher JF, Schlegel HB, Mobashery S. 2005. Ab initio QM/MM study of class A β-lactamase acylation: dual participation of Glu166 and Lys73 in a concerted base promotion of Ser70. J Am Chem Soc 127:15397–15407. https://doi.org/10.1021/ja051592u.
45. Strynadka NC, Adachi H, Jensen SE, Johns K, Sielecki A, Betzel C, Sutoh K, James MN. 1992. Molecular structure of the acyl-enzyme intermediate in β-lactam hydrolysis at 1.7 Å resolution. Nature 359:700. https://doi.org/10.1038/359700a0.
46. Philippon A, Slama P, Dény P, Labia R. 2016. A structure-based classification of class A beta-lactamases, a broadly diverse family of enzymes. Clin Microbiol Rev 29:29–57. https://doi.org/10.1128/CMR.00019-15.
47. Palzkill T, Le QQ, Venkatachalam KV, LaRocco M, Ocera H. 1994. Evolution of antibiotic resistance: several different amino acid substitutions in an active site loop alter the substrate profile of β-lactamase. Mol Microbiol 12:217–229. https://doi.org/10.1111/j.1365-2958.1994.tb01011.x.
48. Petrosino JF, Palzkill T. 1996. Systematic mutagenesis of the active site omega loop of TEM-1 beta-lactamase. J Bacteriol 178:1821–1828. https://doi.org/10.1128/jb.178.7.1821-1828.1996.
49. Therrien C, Sanschagrin F, Palzkill T, Levesque RC. 1998. Roles of amino acids 161 to 179 in the PSE-4 Ω loop in substrate specificity and in resistance to ceftazidime. Antimicrob Agents Chemother 42:2576–2583. https://doi.org/10.1128/AAC.42.10.2576.
50. Doucet N, Wals P-Y D, Pelletier JN. 2004. Site-saturation mutagenesis of Tyr105 reveals its importance in substrate stabilization and discrimination in TEM-1 β-lactamase. J Biol Chem 279:46295–46303. https://doi.org/10.1074/jbc.M407606200.
51. Doucet N, Pelletier JN. 2007. Simulated annealing exploration of an active-site tyrosine in TEM-1 β-lactamase suggests the existence of alternate conformations. Proteins 69:340–348. https://doi.org/10.1002/prot.21485.
52. Doucet N, Savard P-Y, Pelletier JN, Gagné SM. 2007. NMR investigation of Tyr105 mutants in TEM-1 β-lactamase dynamics are correlated with function. J Biol Chem 282:21448–21459. https://doi.org/10.1074/jbc.M609777200.
53. Abriata LA, Palzkill T, Dal Peraro M. 2015. How structural and physicochemical determinants shape sequence constraints in a functional enzyme. PLoS One 10:e0118684. https://doi.org/10.1371/journal.pone.0118684.
54. Abriata LA, Bovigny C, Peraro MD. 2016. Erratum to: Detection and sequence/structure mapping of biophysical constraints to protein variation in saturated mutational libraries and protein sequence alignments with a dedicated server. BMC Bioinformatics 17:439. https://doi.org/10.1186/s12859-016-1315-z.
55. Oteri F, Nadalin F, Champeimont R, Carbone A. 2017. BIS2Analyzer: a server for co-evolution analysis of conserved protein families. Nucleic Acids Res 45:W307–W314. https://doi.org/10.1093/nar/gkx336.

Downloaded from http://mbio.asm.org/ on April 15, 2021 by guest